PROOF COPY 004104GTP

Air Entrainment Versus Lubricant Vaporization in Squeeze Film Dampers: An Experimental Assessment of Their Fundamental Differences

S. E. Diaz

L. A. San Andrés

Mechanical Engineering Department,
Texas A&M University,
College Station, TX 77843-3123

Squeeze film dampers (SFDs) provide structural isolation and energy dissipation in air-breathing engines and process gas compressors. However, SFDs are prone to develop a flow regime where the ingestion of air leads to the formation of a bubbly lubricant. This pervasive phenomenon lacks proper physical understanding and sound analytical modeling, although actual practice demonstrates that it greatly reduces the damper force response. Measurements of film pressures in a test SFD describing circular centered orbits at whirl frequencies varying from 0 to 100 Hz are presented for fully flooded and vented discharge operating conditions. The experiments demonstrate that operation with low levels of external pressurization, moderate to large whirl frequencies, and lubricant discharge to ambient leads to the entrapment of air within the damper film lands. The experiments also elucidate fundamental differences in the generation of film pressures and forces for operation in a flooded condition that evidences vapor cavitation. Damping forces for the vented end with air entrainment are just 15 percent of the forces measured for the flooded damper. Further measurements at constant whirl frequencies demonstrate that increasing the lubricant pressure supply retards the onset of air entrainment. Classical fluid film cavitation models predict well the pressures and forces for the lubricant vapor cavitation condition. However, prevailing models fail to reproduce the dynamic forced response of vented (open-ended) SFDs where air entrainment makes a foamy lubricant, which limits severely the damper film pressures and forces.
[DOI: 10.1115/1.1383258]

PROOF COPY SUBJECT TO CHANGE

Introduction

Excessive steady state synchronous vibration levels and subharmonic rotor instabilities are the two most common problems in rotordynamics. Squeeze film dampers (SFDs) are to date the only effective means to provide structural isolation and vibration dissipation in air breathing engines ([1]). An SFD comprises a thin lubricant film within the annular gap between a non-rotating journal and a stationary housing. The journal is typically connected to the rotor shaft through a ball bearing, though any other type of bearing can be used ([2]). When the rotor vibrates, the journal is forced to follow its whirling motion, thus squeezing the lubricant film. The fluid film develops hydrodynamic pressures in the zones where the film thickness locally decreases. However, when the local film thickness increases the lubricant flow may generate suction (negative dynamic) pressures that may lead to lubricant vaporization or air entrainment.

The Reynolds lubrication equation for incompressible fluids is hitherto used to predict the pressure field in hydrodynamic bearings, including SFDs ([3]). However, Childs [1] Walton et al. [4], and Zeidan and Vance [5,6] establish that the correlation between theory and experiment is considerably less compelling for dampers than for bearings due to the appearance of dynamic lubricant cavitation. It is customarily assumed that, since an ideal fluid is unable to sustain tension, the lubricant would undergo an instantaneous phase change once the fluid vapor pressure is reached. As a result, a vapor filled cavity interrupting the continuity of the film develops. Numerous physical models address the phenomenon of vapor cavitation with different levels of complexity. Braun and Hendricks [7], and Ku and Tichy [8] review these models as applied to the Reynolds equation with boundary conditions defining the onset of cavitation and the full film reformation zone. The simplest model, the half-Sommerfeld or π-film condition, replaces with a uniform (cavitation) pressure any negative pressure resulting from solution of the Reynolds equation. Next, the Swift-Stieber (or Reynolds) condition enforces a null pressure gradient at the cavitation inception boundary to account for flow continuity. The separation model, and the Floberg and Jakobsson-Floberg-Olsson models account for mass transport across the cavitation zone and allow for the occurrence of subambient pressures within the thin fluid film. These models differ from each other in the assumptions about the path followed by the fluid through the cavitation zone.

Zeidan and Vance [9–11] Walton et al. [4] and Hibner and Bansal [12] report a different film rupture mechanism in open-ended squeeze film dampers, as it occurs when the relative movement between the SFD journal and housing drags air into the film eventually leading to a bubbly mixture. Many authors refer to this phenomenon as gaseous cavitation. However, this term is a misnomer strictly applicable to instances where dissolved gases in the lubricant come out of solution at pressures below the saturation value for the noncondensable gas (air), thus forming a single large bubble. In SFDs, as well and in dynamically loaded journal bearings, the bubbly flow due to air entrainment forms a homogeneous mixture with small bubbles well dispersed throughout the film and persisting even in the high pressure zones. (Dowson and Taylor

Contributed by the International Gas Turbine Institute (IGTI) of THE AMERICAN SOCIETY OF MECHANICAL ENGINEERS for publication in the ASME JOURNAL OF ENGINEERING FOR GAS TURBINES AND POWER. Paper presented at the International Gas Turbine and Aeroengine Congress and Exhibition, Indianapolis, IN, June 7–10, 1999; ASME Paper 99-GT-187. Manuscript received by IGTI Oct. 1998; final revision received by the ASME Headquarters Mar. 1999. Associate Editor: D. Wisler.

Copyright © 2001 by ASME

PROOF COPY 004104GTP

[13], Jacobson and Hamrock [14], Zeidan and Vance, [5,9] Sun et al. [15]. Foamy off at the damper outlet evidences this pervasive operating condition.

Zeidan et al. [2] review the state of the art in SFDs and remark about the importance of the air entrainment phenomenon, as it considerably reduces the dynamic film forces and the overall damping capability of SFDs. There are no accurate models addressing to the effects of air ingestion in dynamically loaded bearings and SFDs, nor are there relevant experimental measurements that could aid in validating predictive analysis. Only recently, Diaz and San Andrés [16–18] provide experimental results on a test SFD describing circular centered orbits and correlate dynamic pressures and squeeze film forces to the volume concentration of air in a controlled bubbly mixture. The experiments evidence a dramatic reduction in film pressures and forces as the air volume fraction increases in the mixture.

The experimental results hereby presented evidence the paramount effect of air entrainment in the performance of SFDs operating with an open-end to ambient discharge, the most common configuration found in practical applications. The measurements evidence the fundamental differences in film pressure generation and forces for operation with a vented end versus a fully flooded condition where lubricant vaporization prevails. The test results also demonstrate the similarity between the dynamic pressure fields generated by air entrainment and those measured for operation with a controlled homogeneous bubbly mixture. The effect of increased supply pressure and lubricant through flow on the delay of air entrainment within the fluid film is also investigated.

Test Fig Description

The experiments are conducted in an open-ended damper operating with a circular centered whirl orbit of amplitude equal to 50 percent of the film clearance. Diaz and San Andrés [16–18] describe the test apparatus, measurement procedure and uncertainty analysis. Figure 1 depicts the damper test section, flow loop, instrumentation and relevant nomenclature. The damper journal diameter (D) and axial length (L) are equal to 129.4 mm and 31.1 mm, respectively. The journal and its ball bearing are mounted eccentrically on a rigid shaft. A variable-speed DC motor and belt transmission drive the shaft supported on two precision ball bearings. At a pressurized condition of 7.0 bar the nominal radial clearance (c) and orbit radius (e) are equal to 0.343 mm and 0.216 mm, respectively. The left end of the damper is tightly sealed with an O-ring, while its right end opens to an exit plenum at ambient pressure. The lubricant enters the damper through two holes at the top (90 deg) and bottom (270 deg) of the damper left end.

The experiments are performed with an ISO VG 68 pure lubricant of density and viscosity equal to 0.87 gr/cm^3 and 77.5 centipoise at 28°C, respectively. The lubricant is delivered to the test section via a gear pump and removed from the discharge plenum with an auxiliary pump. The lubricant flow rate and supply pressure are recorded at the inlet port with a gear flowmeter and a Bourdon-type pressure gauge, respectively. A K-type thermocouple detects the lubricant film temperature, a photoelectric tachometer senses the drive shaft speed (equal to the journal whirl frequency), and two eddy current displacement sensors record the motion of the journal. Six piezoelectric dynamic pressure sensors are flush mounted around the damper circumference at two axial planes (Z_1 and Z_2) as depicted in Figs. 1(a,b).

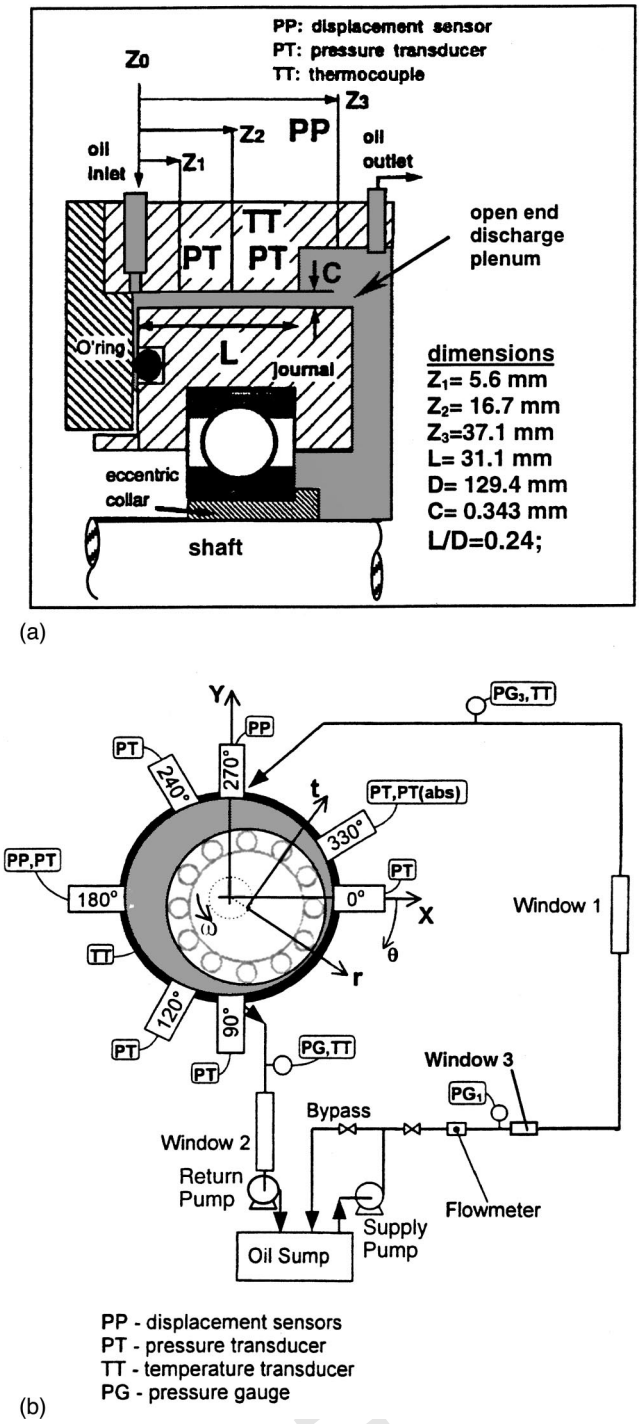

Fig. 1 Test apparatus; (*a*) squeeze film damper detail, (*b*) schematic of test rig and instrumentation

Experimental Procedure

The lubricant supply pressure and flow rate, film temperature, and synchronous whirl frequency are manually recorded in the experiments. The dynamic film pressure at the location (180 deg, Z_2), see Fig. 1, is measured with a piezoelectric transducer and digitally recorded with 16 bits of resolution at a sampling rate of 2048 Hz for a total length of 2 sec.

Four types of experiments have been conducted to evaluate the performance of the test SFD under different operating conditions. Measurements of the pressure field and film forces are performed for fully flooded and open-end vented conditions and for increasing whirl frequencies while maintaining the same supply pressure. In the first type of measurements, the damper discharge plenum is fully flooded with lubricant at atmospheric pressure preventing the ingestion of external air. In this case, the fluid in the damper film lands shows vapor cavitation while the damper operates at a given whirl frequency. The second type of measurements exemplifies a more realistic operating condition where the lubricant discharges to an open plenum vented to atmospheric conditions. In this case

air entrains naturally into the squeeze film lands and the discharged lubricant has the appearance of a bubbly mixture resembling a foamy fluid.

In the measurements with increasing whirl frequencies, the supply pressure is set to a constant value of 2.3 bar, which corresponds to a lubricant flow rate of 0.4 l/min. In the vented to ambient condition tests the lubricant is evacuated from the plenum discharge chamber using a small diaphragm pump sectioning at a bottom port. On the other hand, the whole damper test section is submerged in a lubricant bath for the flooded condition tests. In this last case, the lubricant is evacuated from a top port directly to the oil sump. The plenum pressure is at atmospheric pressure for both test conditions. A transparent window on the damper housing discharge section allows verifying that the plenum remains either fully flooded or empty, depending on the type of test conducted. The SFD rig is brought rapidly to a maximum shaft speed of 6,000 rpm (100 Hz), and the measurements are performed while reducing the speed by steps of 500 rpm (8.33 Hz) each.

The other two types of measurements illustrate the performance of the open-end vented SFD for different lubricant flow rates (pressure supplies) and operating at two whirl frequencies, 8.33 Hz (500 rpm) and 16.67 Hz (1000 rpm). The measurements are performed while the supply pressure (or oil through flow) is increased in discrete steps until the return auxiliary pump is not able to evacuate all the lubricant and the discharge plenum starts to overflow.

The manufacturer values for the uncertainty of the measurement sensors have been verified. The individual errors are 1 percent of measurement for the oil flowmeter 3 percent of full scale (10.3 bar) for the Bourdon pressure gauge, and 1 percent of full scale (100°C) for the thermocouples. The instrumentation uncertainty on the dynamic pressure measurements is mainly related to the A/D conversion, which is on the order of hundredths of a bar. However, the large temporal fluctuations of the pressures introduce a first-order uncertainty ([19]) that overcomes the instrumentation uncertainty by about two orders of magnitude. The discussion of test results addresses at length this issue.

Experimental Results

Figure 2 depicts the measured squeeze film pressures for the fully flooded and vented operating conditions. The solid lines represent the dynamic pressures and the dotted lines show the variation of the film thickness at the location of measurement and for five periods of journal whirl motion. In both tests, the supply pressure is 1.45 bar and the discharge plenum is nearly at atmospheric pressure. The oil flow rate is 0.12 liter/min and the film temperature is 27°C. The SFD journal describes circular centered orbits with an orbit radius of 0.180 mm at a whirl frequency of 75 Hz.

Figure 2(*a*) shows the typical pressure profile found when the pure lubricant undergoes a vapor cavitation process. Note that the pressure profile is smooth and shows nearly identical shapes for each period of motion. A (flat) constant pressure zone develops at nearly zero absolute pressure, and it corresponds to the rupture of the film and formation of a vapor filled cavity. The vapor cavity appears only during that portion of the journal motion cycle where the film gap increases. The vapor bubble collapses immediately as the local pressure raises above the lubricant vapor pressure. In general, correlations of measured pressures and vapor cavitation extent with predictions based on traditional film rupture models are satisfactory.

The pressure profile shown in Fig. 3(*b*) shows the effects of air entrainment for the vented to ambient condition. The periodic motion of the journal not only squeezes the lubricant but it also induces air ingestion and entrapment. At the times when the local film gap increases a suction pressure draws air into the thin film and leads to the formation of a bubbly mixture of air in oil, with bubbles persisting even in the high pressure zones. Note that the squeeze film pressures differ markedly for each period of journal

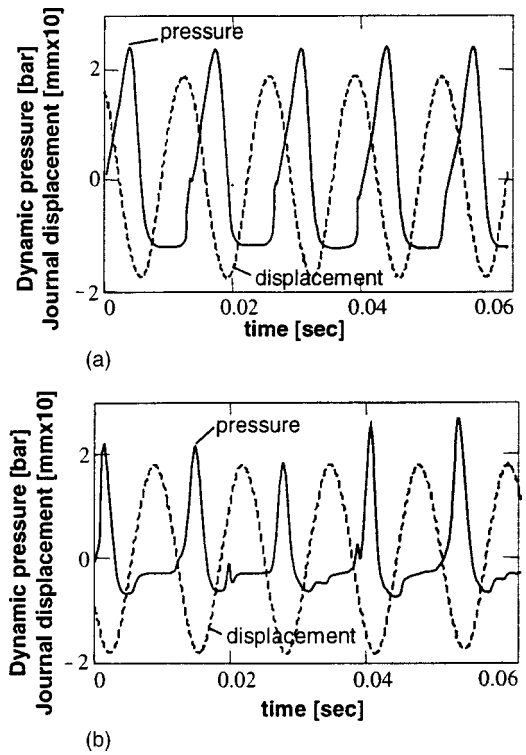

Fig. 2 Dynamic pressure and journal displacement versus time; (*a*) flooded plenum and (*b*) vented plenum

motion and even the peak pressures undergo large variations. A pressure flat zone at nearly ambient pressure, typically denoted as gaseous cavitation, initiates when the film goes from its minimum to its maximum values (negative squeeze action). The generation of subambient film pressures is also unique during the negative squeeze portion of the journal motion cycle.

A period-averaging scheme is applied to the measured pressures to filter random fluctuations, thus generating smooth periodic pressure fields representative of the overall behavior of the squeeze film pressures over many cycles of motion. Figures 3(*a*) and 3(*b*) compile the period-averaged dynamic pressures corresponding to measurements at different operating whirl frequencies for the flooded and vented open end, respectively. The vertical axis represents the pressure, the horizontal axis depicts the time normalized by the period of motion, and the off-plane axis denotes the whirl frequency ranging from 0 to 100 Hz (0–6000 rpm). For the flooded condition and at low whirl frequencies the level of external supply pressure prevents the onset of the fluid vapor cavitation zone. However, as the whirl frequency increases, the dynamic film pressures are low enough and approach the vaporization pressure, thus initiating the vapor cavitation zone. The extent of the vapor cavitation zone increases linearly with the journal whirl frequency.

On the other hand, the dynamic pressures corresponding to operation with a vented discharge condition (Fig. 3(*c*)) are most distinctive and resemble the pressures measured earlier in the same test rig operating with a controlled homogeneous bubbly mixture of air and oil ([16–18]). A constant pressure zone that interrupts the pressure rise from the minimum to the maximum peak develops and with a magnitude nearly equal to the ambient pressure. The extent of the flat pressure zone increases rapidly with the whirl frequency for low frequencies. However, as the operating frequency increases further, the extent of the constant pressure zone appears nearly constant. Diaz and San Andres [16,18] have correlated the extent of the constant pressure zone with the concentration of air in a test SFD operating with a controlled homogeneous bubbly mixture. Thus, the extent of the flat

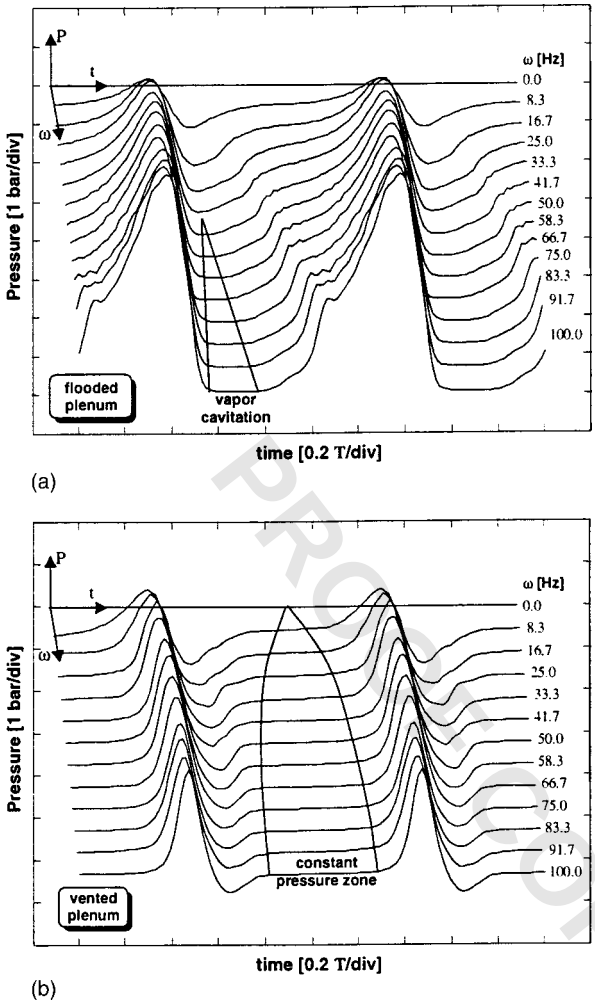

Fig. 3 Development of the period-averaged pressure field and uniform pressure zone versus shirl frequency (flooded and vented end conditions); (*a*) flooded plenum, (*b*) vented plenum

pressure zone in the current measurements denotes increasing degrees of air entrainment as the whirl frequency increases.

Figure 4 provides a quantitative comparison of the peak-to-peak (p-p) pressures generated by the test SFD operating with vapor cavitation (flooded plenum) and with air entrapment (vented open end). The magnitude of the p-p pressures for the vented condition represents an averaged value from the many periods of measurement. The vertical bars represent the first-order uncertainty as defined by Moffat [19], i.e., they correspond to the largest deviations (above and below) from the average value for the entire length of

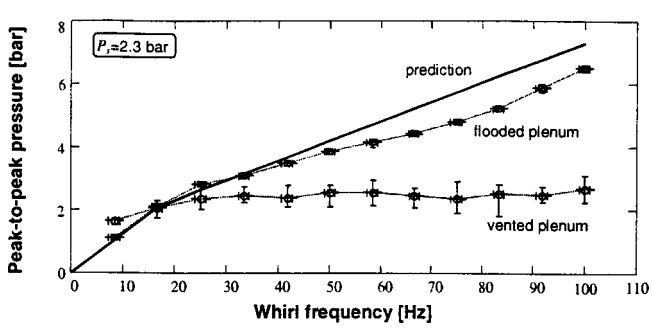

Fig. 4 Peak-to-peak pressure versus whirl frequency (flooded and vented end conditions and predictions

the experiment. Figure 4 also includes an analytical prediction of the p-p pressures and based on the simplest model available, the short length bearing with open ends, and given as

$$P_{\text{short}}=\frac{6\mu e\omega}{h^3}\sin(\theta)(Z^1-L^2)+P_o \tag{1}$$

and accounting for vapor cavitation with the simple relation

$$P=\begin{cases} P_{\text{short}} & \text{if } P_{\text{short}}>0 \\ 0 & \text{if } P_{\text{short}}\leqslant 0 \end{cases}. \tag{2}$$

Refer to the Nomenclature for a proper definition of all variables.

The short length bearing model predicts a linear growth of the p-p pressures with the journal whirl frequency. The rate of p-p pressure rise reduces above the whirl frequency at which the lubricant vapor cavitation initiates (~17 Hz). The experimental pressures for the flooded SFD condition correlate very well with the predicted values. However, the p-p pressures for the vented condition quickly reach a constant value, (nearly) independent of the whirl frequency and much lower than for the flooded condition. The first-order uncertainties for the flooded condition are rather small indicating a time invariant pressure field. On the other hand, the tests with air ingestion and entrapment lead to p-p pressure fluctuations of up to 35 percent.

A SFD describing circular centered orbits and with a stationary[1,2] pressure field (synchronous with the shaft) generates invariant forces in a radial and tangential coordinate system rotating with the same speed as the shaft. A pure tangential force is distinctive of an ideal SFD since this force directly opposes any forward whirl motion. Radial forces could be centering denoting a stiffness-like effect, or outwards implying a fluid inertia effect. Dynamic damper forces (f_r, f_t) in the radial and tangential directions arise from integration of the pressure field around the journal surface. A kinematic relation between the *stationary* (though rotating) pressure field and the *dynamic* pressure field at a fixed location is used to transform the spatial integration around the journal circumference into integration in time. The relationship is

$$f_{(Z)}=(f_r+i\cdot f_t)_{(Z)}=\frac{-\omega\frac{D}{2}}{n}\int_{to}^{to+n\cdot T}P_{(t,z)}\cdot e^{-i\cdot[e(t-t_0)]}dt. \tag{3}$$

Refer to the Nomenclature for a proper definition of all variables.

Figure 5 depicts the radial and tangential forces per unit length at the axial location of measurement (Z_2) versus the journal whirl frequency. Circles and squares denote the measured forces for the vented and flooded conditions, respectively, and solid lines represent the forces predicted by the short length bearing model. Note that the radial forces are much lower than the tangential (damping) forces. The analytical predictions show the damping force to increase linearly with the whirl frequency, although with a reduced slope after vapor cavitation initiates. The calculated radial force is nil for a full-film condition, and increases linearly with the whirl frequency after vapor cavitation initiates. The predictions agree well with the forces derived from the experimental pressures under a flooded discharge operating condition. Conversely, for the vented plenum and where air entrains naturally into the fluid film, the damping (tangential) force actually decreases as the whirl frequency increases and becomes a mere fraction (15 percent) of the damping force obtained for the flooded SFD condition. At large whirl frequencies when air entrainment is more severe; the radial force becomes larger than the tangential force.

Figure 6 demonstrates the effects of the supply pressure (lubricant flow rate) on the generation of film pressures and the onset of air entrainment. Figure 6(*a*) compiles the period averaged pressures at an operating frequency equal to 16.67 Hz (1000 rpm), and

[1]Here the stationary qualification means an invariant pressure field relative to an observer positioned in the spinning shaft.

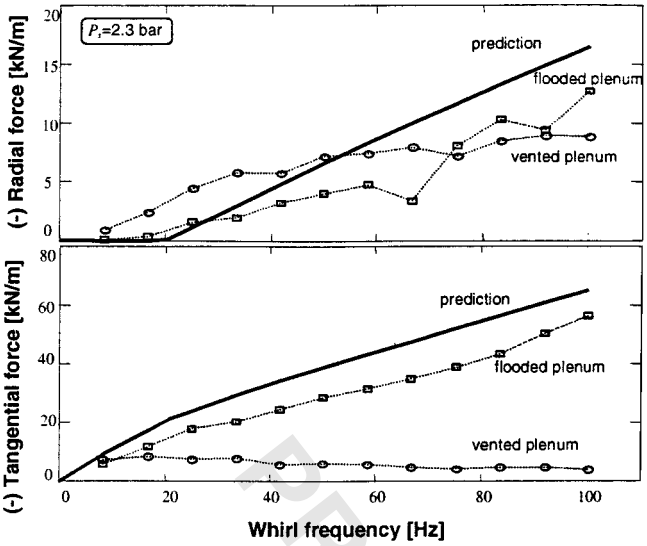

Fig. 5 Radial and tangential forces versus whirl frequency (flooded and vented end conditions and predictions)

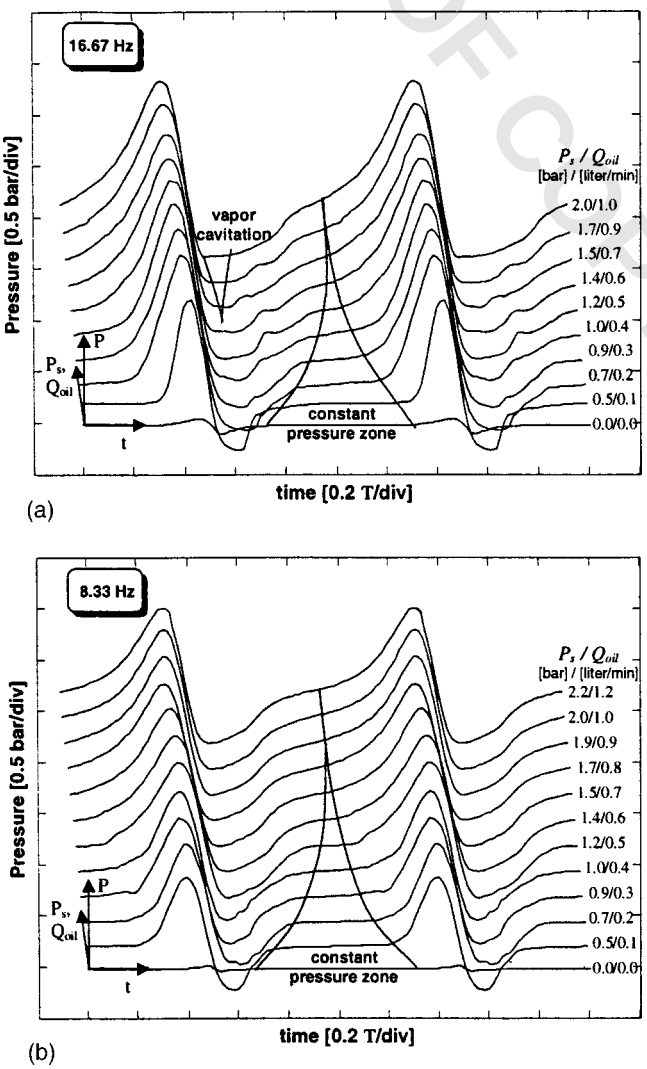

Fig. 6 Development of the period-averaged pressure field and uniform pressure zone versus the lubricant flow and supply pressure; (*a*) whirl frequency 16.67 Hz (1000 rpm), (*b*) whirl frequency 8.33 Hz (500 rpm)

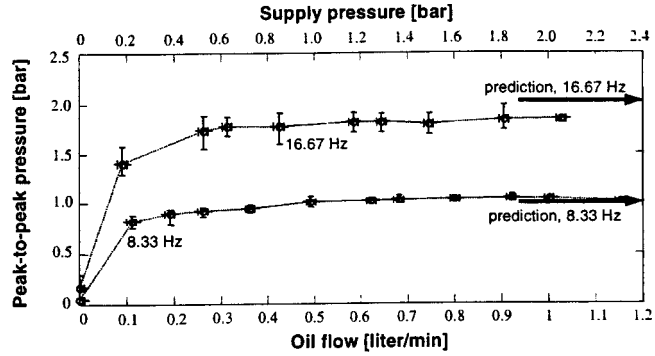

Fig. 7 Peak-to-peak pressures versus oil flow rate and supply pressure for two whirl frequencies

Fig. 6(*b*) depicts the pressures at 8.33 Hz (500 rpm). The SFD discharge plenum is vented to atmospheric pressure. In the figures, the vertical axis represents the pressure, the horizontal axis depicts the time normalized by the period of motion, and the in-plane axis gives the magnitude of supply pressure and lubricant flow rate. The measurements evidence that increasing the lubricant through flow rate reduces the extent of the constant pressure zone where air is entrapped. That is, the severity of air entrainment decreases allowing for the generation of larger squeeze film pressures and fluid film forces. Note that in the tests at 16.67 Hz, a lubricant vapor cavitation zone starts to develop for the largest flow rates.

Figure 7 depicts the period averaged *p-p* pressures corresponding to the dynamic pressures shown in Fig. 6 versus the oil flow rate and the supply pressure. The figure also includes the predicted theoretical values derived from the short bearing model given by Eq. (2). For both operating whirl frequencies, the *p-p* pressure grows rapidly with the supply pressure. For large flow rates the *p-p* pressures approach an asymptotic value, and correlate well with the simple analytical values. Note that the theoretical model does not predict fluid vaporization or air entrainment at these low frequencies. The experiments also evidence that larger lubricant flow rates are needed to control air entrainment as the whirl frequency increases.

Figure 8 depicts the test radial and tangential forces versus the oil flow rate and supply pressure for the whirl frequencies equal to

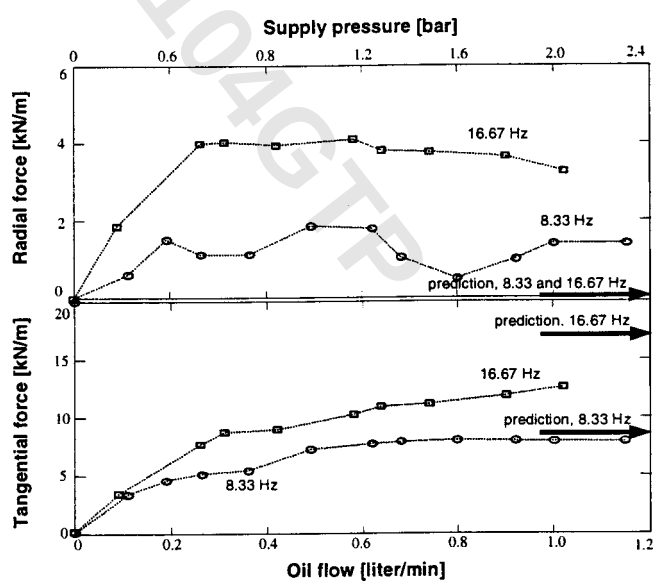

Fig. 8 Radial and tangential forces versus oil flow rate (supply pressure) for two whirl frequencies

8.33 and 16.67 Hz. The experiments at the lower whirl frequency reveal a rapid increase of the tangential film force towards the analytical asymptotic value. However, at the whirl frequency of 16.67 Hz, the tangential (damping) force grows continuously within the full range of test supply pressures. Unfortunately, the current test facility does not allow for higher levels of pressurization so it is not possible to confirm the asymptotic trend of the tangential force for large flow rates. The radial forces are small and appear to decrease with the supply pressure for the higher test whirl frequency (16.67 Hz). Note that in practice, higher supply pressures are not readily available nor are desired because of the increased cost and bulky hardware.

Conclusions

The force response of squeeze film dampers is affected by numerous factors, including geometric characteristics, lubricant type, whirl frequency, and supply and discharge mechanisms. Ingestion and entrapment of air is pervasive in SFDs operating with vented open ends at ambient pressure. The fluid film becomes a foamy-like mixture with air bubbles persisting in the regions of pressure generation above ambient. Current models for the rupture of thin films, gaseous and vapor cavitation, are strictly applicable for static loads, and their extension to transient or periodic loads gives accurate predictions only for bearings fully submerged in a lubricant bath.

Experiments have been conducted on a controlled orbit test SFD operating with two end conditions, one is fully flooded with lubricant, and the other one is just an open vent to ambient as most typical applications exemplify. Measurements of the dynamic film pressures and estimated fluid film forces are performed for increasing whirl frequencies at a fixed value of supply pressure. In the flooded SFD the film pressures are quasi-stationary and repetitive for each cycle of damper motion, and where the lubricant vapor cavitation zone increases linearly with the journal whirl frequency. On the other hand, for the vented condition, and as soon as air is ingested into the film lands, the film pressures show random variations and sudden spikes, zones of subambient pressures, and a discharge fluid appearing as a bubbly mixture. A constant pressure zone at ambient pressure also grows linearly with the whirl frequency.

Period-averaged peak-to-peak (p-p) pressures and film forces are calculated from the measured pressure fields. For the flooded condition, the p-p pressure increases linearly with the journal whirl frequency, and its rise rate reduces at the frequency where lubricant vapor cavitation initiates. The damping (tangential) force shows a similar trend. A radial (centering) force also appears when the fluid cavitates and its magnitude is proportional to the whirl frequency. In contrast, with a vented plenum condition, the p-p pressures quickly reach a constant value, (nearly) independent of the journal whirl frequency and much lower than for the flooded condition. The damping force actually decreases as the whirl frequency increases, and becomes a mere fraction ($\sim$15 percent) of the tangential force obtained from the flooded condition. At large whirl frequencies when air entrainment is more severe; the radial force becomes larger than the tangential force. Theoretical predictions based on a classical model predict well the pressures and forces for the flooded condition (vapor cavitation), but fail to reproduce the test values for the vented condition which develops into a foamy-like mixture.

Further experiments at low whirl frequencies demonstrate that increasing the supply pressure reduces the extent of air entrainment and increases the film p-p pressures and damping forces. However, the beneficial effect of external pressurization becomes less pronounced as the frequency of operation increases. A sound theoretical model accounting for air entrainment is needed for the reliable design of SFDs, thus reducing their costly trial and error tuning process. The test results suggest that considering the squeeze film flow as a homogeneous continuous mixture could lead to improved predictive analysis. Recently, Tao et al. [20] present an initial model that compares favorably with controlled mixture *SFD* test results, though it requires of an empirical formulation for the bubbly fluid viscosity. Diaz [21] also offers another perspective to the analysis and presents a simple model, verified by the measurements, to predict the onset and extent of air entrainment and its paramount effect on *SFD* forced performance.

Acknowledgments

The support of the TAMU Turbomachinery Research Consortium is gratefully acknowledged. The first author thanks the financial aid from CONICIT (Consejo Nacional de Investigaciones Científicas y Tecnlógicas) and Universidad Simón Bolívar, Venezuela.

Nomenclature

C = damper radial clearance (0.343 mm)
D = journal diameter (129.4 mm)
e = journal orbit radius, nominal value (0.216 mm)
f_r, f_t = radial and tangential film forces per unit length (N/m)
h = film thickness, $C+e\cos(\omega t)$
i = $\sqrt{-1}$ imaginary unit
L = journal length (31.1 mm)
P = film pressure (bar)
P_o, P_s = exit plenum pressure (1.0 bar); supply pressure (bar)
P_{short} = short length bearing solution for squeeze film pressure
Q_{oil} = oil flow rate (liters/min)
r, t = radial and tangential coordinates
t = time (sec)
t_o = time for minimum film thickness (sec)
T = $2\pi/\omega$; period of journal motion (sec)
Z_j = axial location of pressure measurements; Z_1 (5.16 mm), Z_2 (16.7 mm)
μ = lubricant viscosity
θ = angular coordinate in a rotating reference frame
ω = journal whirl frequency (rad/sec)

References

[1] Childs, D., 1993, *Turbomachinery Rotordynamics*, John Wiley and Sons, New York.
[2] Zeidan, F. Y., Vance, J. M., and San Andrés, L. A., 1996 "Design and Application of Squeeze Film Dampers in Rotating Machinery," *Proceedings of the 25th Turbomachinery Symposium*, Texas A&M University, College Station, TX, pp. 169–188.
[3] Vance, J. M., 1988, "Rotordynamics of Turbomachinery," John Wiley and Sons, New York.
[4] Walton, J., Walowit, E., Zorzi, E., and Schrand, J., 1987, "Experimental Observation of Cavitating Squeeze Film Dampers," ASME J. Tribol., **109**, pp. 290–295.
[5] Zeidan, F. Y., and Vance, J. M., 1989, "Experimental Investigation of Cavitation Effects on The Squeeze Film Force Coefficients," *Rotating Machinery Dynamics*, DE-Vol. 18-1, ASME, New York, pp. 237–242.
[6] Zeidan, F. Y., and Vance, J. M., 1990, "A Density Correlation for a Two-Phase Lubricant and its Effect on the Pressure Distribution," STLE Tribol. Trans., **33**, pp. 641–647.
[7] Braun, M. J., and Hendricks, R. C., 1984, "An Experimental Investigation of the Vaporous/Gaseous Cavity Characteristics of an Eccentric Journal Bearing," ASLE Trans., **27**, No. 1, pp. 1–14.
[8] Ku, C. P., and Tichy, J. A., 1990, "An Experimental and Theoretical Study of Cavitation in a Finite Submerged Squeeze Film Damper," ASME J. Tribol., **112**, pp. 725–733.
[9] Zeidan, F. Y., and Vance, J. M., 1989, "Cavitation Leading to a Two Phase Fluid in a Squeeze Film Damper," STLE Tribol. Trans., **32**, No. 1, pp. 100–104.
[10] Zeidan, F. Y., and Vance, J. M., 1990, "Cavitation Regimes in Squeeze Film Dampers and Their Effect on the Pressure Distribution," STLE Tribol. Trans., **33**, pp. 447–453.
[11] Zeidan, F. Y., and Vance, J. M., 1990c, "Cavitation and Air Entrainment Effects on the Response of Squeeze Film Supported Rotors," ASME J. Tribol., **112**, pp. 347–353.
[12] Hibner, D., and Bansal, P., 1979, "Effects of Fluid Compressibility on Viscous Damper Characteristics," *Proc. Conf. on the Stability and Dynamic Response of Rotors with Squeeze Film Bearings*. University of Virginia, Charlottesville, VA, pp. 116–132.

PROOF COPY 004104GTP

PROOF COPY 004104GTP

[13] Dowson, D., Godet, M., and Taylor, C. M., 1974, eds, *Cavitation and Related Phenomena in Lubrication*, ImechE, London.
[14] Jacobson, B. O., and Hamrock, B. J., 1983, ''High-Speed Motion Picture Camera Experiments of Cavitation in Dynamically Loaded Journal Bearings,'' ASME J. Tribol., **105**, pp. 446–452.
[15] Sun, D. C., Brewe, D. E., and Abel, P. B., 1993, ''Simultaneous Pressure Measurement and High-Speed Photography Study of Cavitation in a Dynamically Loaded Journal Bearing,'' Trans. ASME, **115**, pp. 88–95.
[16] Diaz, S. E., and San Andrés, L., 1998, ''Measurements of Pressure in a Squeeze Film Damper With an Air/Oil Bubbly Mixture,'' STLE Tribol. Trans., **41**, No. 2, pp. 282–288.
[17] Diaz, S., and San Andrés, L., 1998b, ''Reduction of the Dynamic Load Capacity in a Squeeze Film Damper Operating with a Bubbly Lubricant,'' ASME Paper 98-GT-109.
[18] Diaz, S., and San Andrés, L., 1998c, ''Effects of Bubbly Flow on the Dynamic Pressure Fields of a Test Squeeze Film Damper,'' ASME Paper FEDSM98-5070.
[19] Moffat, R. J., 1982, ''Contributions to the Theory of Single-Sample Uncertainty Analysis,'' ASME J. Fluid Eng., **104**, pp. 250–260.
[20] Tao, L., Diaz, S., San Andrés, L., and Rajagopal, K., 1998, ''Flow Analysis of Squeeze Film Dampers Operating With Bubbly Lubricants,'' TAMU Turbomachinery Research Consortium Progress Report, TRC-SFD-1-98, College Station, TX, May.
[21] Diaz, S. E., 1999, ''The Effect of Air Entrainment on the Forced Response of Squeeze Film Dampers: Experiments and Analysis,'' Ph.D. dissertation, Mechanical Eng. Dept. Texas A&M University, May.

PROOF COPY 004104GTP

PROOF COPY 004104GTP